Engineered Science
DOI: https://dx.doi.org/10.30919/es1253

Vibrational Behavior and Dynamic Analysis of Cracked Rotor Systems during Transient Conditions

Saad S. Alkhfaji[1, 2,*]

Abstract

The rotating shafts are an essential part of any rotating machinery. Their dynamic behavior usually receives substantial care in the design stage of rotating machines, especially when the presence of cracks is taken into account. The purpose of this paper is to investigate numerically and experimentally the influence of transverse cracks in rotating shafts on rotor dynamic behavior during transient conditions. The work comprises developing a displacement-based finite element model for the cracked rotor to generate its dynamic characteristics represented in vibration transient response, natural frequency, and critical speed. Various crack depths located at different positions along the rotor were considered when designing the numerical model. A numerical example was utilized to verify the validity of the developed model. In addition, an experimental apparatus was arranged to validate the developed computational model. The results obtained indicate that the presence of crack leads to a remarkable change in vibration response, natural frequency, and critical speed. The amount and nature of this change were observed to vary with crack depth and location. Consequently, a novel model is proposed in this paper that suggests a possible approach for an online monitoring and diagnostic method for rotating machines.

Keywords: Cracked rotor; Rotating machine; Rotors; Critical speed; Dynamic behavior.
Received: 22 February 2024; Revised: 30 May 2024; Accepted: 05 June 2024.
Article type: Research article.

1. Introduction

Rotating shafts are essential elements of modern applications in mechanical engineering. Rotating machinery, such as turbines, compressors, pumps, jet engines, *etc*., are imposed on variable loading conditions. Consequently, the crack occurrence is unavoidable. Therefore, it is of great importance to study the dynamic of cracked rotating shafts as the development and propagation of the crack often lead to rotor failure in real-life operation conditions. Rotor failure occurs when the remaining cross-section of the shaft that is not damaged by the crack becomes insufficient to tolerate the applied loading. A rapid failure occurs when the critical size of the crack is reached.[1,2]

Cracks, according to their geometries, can be generally categorized into two types, namely transverse and longitudinal cracks. Transverse cracks are usually perpendicular to the rotor shaft axis, while longitudinal cracks are parallel to the shaft axis. The most common and serious cracks are transverse cracks, which weaken the rotating shaft by generating local flexibility in the rotor stiffness by concentrating strain energy in the crack region. Transverse cracks in rotor systems result from cyclic loading and other conditions to which rotating machines are imposed. Therefore, such cracks have been dealt with by a considerable number of researchers.

The issue of modeling a cracked shaft has been an important engineering issue over the past five decades. This is primarily due to the fact that crack occurrence, which may appear in rotors during their operation, results in serious complications and catastrophic accidents if not predicted early. An early crack detection can considerably enhance the durability of rotor systems. The methods of shaft crack modeling can be classified into three main categories. These are local stiffness reduction, complex models in two or three dimensions, and discrete spring models. Modeling cracked rotor dynamics and analyzing their dynamic response are core issues in rotating machinery. In this respect, an appropriate

[1] *Dept. of Mechatronics Engineering, Middle Technical University, Baghdad 10011, Iraq.*
[2] *Dept. of Medical Device Engineering, Ashur University, Baghdad, Postcode 10011, Iraq.*
**Email:* drsaadsmi@mtu.edu.iq, saad.alkhfaji@au.edu.iq (S. S. Alkhfaji)

mathematical model for the cracked rotor is required for accurate prediction of dynamic response. A considerable number of researchers have studied the dynamic behavior of cracked rotors using theoretical and or experimental methods, for example.[3-22] However, most of these studies mainly focus on trying different approaches to assess the dynamic behavior of rotors with crack occurrence, seeking different approaches for crack detection based on the dynamic response. In addition, those researchers have indicated the fact that it is easier to detect cracks while the rotor passes through its critical speed than when at a steady speed.

To the best of our knowledge, little research was found focusing on analyzing the transient response of the multi-disc rotary system with cracks during machine run-up conditions. For example, the work carried out studied the effects of angular acceleration,[23] amplitude of aerodynamic force crack depth, and position on the dynamic characteristics of a cracked compressor blade during the run-up process through the FE model of a rotating compressor blade. They indicated that the crack-induced second- and third-order super-harmonics can be seen and become more evident with increasing crack severity.[24] Experimentally, the dynamic response of a cracked rotor with a breathing crack was studied while passing through subcritical speed, focusing on the dynamic behavior of the orbits and frequency spectra obtained by the FFT method. Their experimental results were compared with the theoretical findings in the literature.[25] In their study, they developed a general equation of motion with the assumption of weight dominance for a Jeffcott rotor with a transverse crack, taking into account the complicated whirl of the rotor. They found that these equations are not suitable for studying the vibration of a cracked rotor near the critical speed.[26] proposed a breathing function to study crack breathing behavior with small cracks existing. They found that the time-frequency representations based on an improved decomposition algorithm can lead to the prediction of smaller cracks.

Therefore, the current research focuses on investigating the dynamic behavior of a multi-disc cracked rotor system during machine running up, considering various crack depths and locations. Timoshenko beam element with two nodes and four degrees of freedom (DOFs) per node was utilized. The effect of gyroscopic moments, translational and rotary inertia, and transverse shear deformations are considered. An equivalent beam element model is employed to introduce the transverse crack on the rotating shaft. In addition, the geometry of the rotary machine and the flexibility of the bearing supports are considered when building the model. Simulations for numerical examples are implemented to analyze the dynamic behavior of the cracked rotor system. The effect of various crack depths and positions on the dynamic properties is investigated in detail. The results of this work may provide guidance for rotating machine designers and health monitoring or diagnosing of rotating machinery.

2. Modeling of rotor system

Modeling and simulation techniques are broadly employed in the design stages and analysis of rotor-bearing systems to perform dynamic analysis for the design of modern machines. Consequently, potential problems can be predicted at an early stage of machine design.[27] A finite element (FE) approach has been adopted to develop a displacement-based computational model to tackle the issue of the dynamic behavior of rotary machines with the presence of cracks. In this section, the modeling procedure is described.

The major component in any rotating machine is the rotor, which generates or transmits power from one place to another. The rotor generally involves a rotating shaft carrying other machine parts like turbine wheels, impeller wheels, and gears. The rotor, in general, is not entirely rigid as, in some cases, it is quite flexible. The rotor can be supported on two or more bearings. Location, stiffness and damping properties of bearings play a significant role in analyzing the dynamic performance of rotor systems.

The rotating shaft was modeled using Timoshenko-type beam in which shear, rotational inertia and effect of gyroscopic couples are considered. Discs which are normally rigid are introduced by mass, polar and diametral mass moments of inertia. Bearings can be modeled using linear springs and dashpots. The rotor-bearing system matrices can be determined via FE modeling procedures.[28]

2.1 Modelling of the cracked beam section

This section describes the modeling of the cracked shaft section. In this study, a simple method is presented to model the transverse crack relying on the fact that the presence of a crack in the shaft reduces the local stiffness of the shaft near the location of the crack and consequently the natural frequency of the original intact shaft will be reduced. The reduction of stiffness is, to some degree, proportional to the depth of the crack. This is usually achieved by reducing the second moment of the area of the shaft cross-section. The transverse crack in a rotating shaft is modeled as a circular segment within the cracked beam element, as shown in Fig. 1. Consequently, the crack influence can be expressed as the reduction in the element's second moment of area at the crack position.

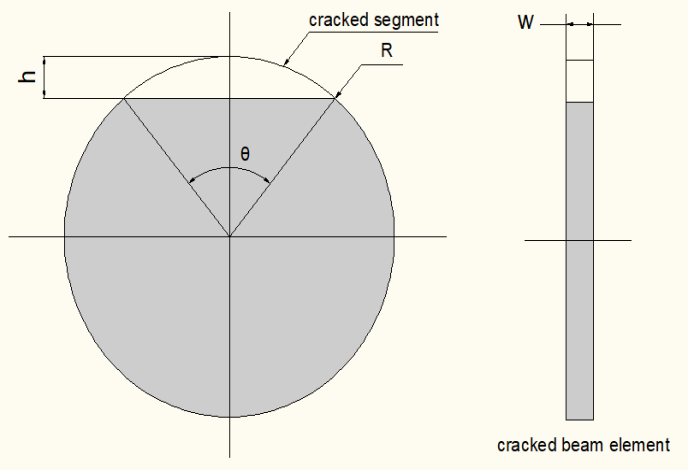

Fig. 1 Modeling of the cracked shaft section.

where h and w refer to the depth and width of the crack, respectively, θ is the angle proportional to crack depth, and R denotes the radius of the shaft.

The angle (θ) can be found as in below:

$$\theta = 2cos^{-1}(1-\frac{h}{R}) \quad (1)$$

Consequently, for a given crack depth, the area of the cracked segment (Acr) can be determined by:

$$Acr = \frac{R^2}{2}(\theta - sin\theta) \quad (2)$$

The moment of inertia of the cracked segment (Icr) can be defined as given below:

$$Icr = \frac{R^4}{4}(\theta - sin\theta + \frac{2}{3}sin\theta sin^2\frac{\theta}{2}) \quad (3)$$

The effective moment of inertia of the cracked beam element (Ie) can then be calculated by:

$$Ie = I_{solid} - Icr \quad (4)$$

where I_{solid} denotes the moment of inertia of the uncracked beam element section.

Similarly, the effective cross-sectional area of the cracked shaft element (Ae) can be determined from:

$$Ae = A_{solid} - Acr \quad (5)$$

Here also, A_{solid} describes the cross-sectional area of the uncracked beam element section.

2.2 Developing the global matrices of a multi-disc cracked rotor system

The finite element (FE) method is an effective tool to model rotating machine dynamics, taking into account the flexibilities of all rotating components, and has been largely used for rotor dynamics design to provide the mathematical representation of the rotating machines. This section presents the development and assembling of the global mass, damping, and stiffness matrices of multi-disc rotary systems. The dynamic responses can then be comprehensively identified via determining the natural frequencies and mode shapes using the global matrices developed for the rotor-bearing system.[28]

In the modeling procedure, the rotating shaft is divided into a number of Timoshenko beam finite elements.[27] Each beam element is expressed as an element with two nodes. Four degrees of freedom, in the lateral direction, two translations, and two rotations, are introduced for each node as demonstrated in Fig. 2.

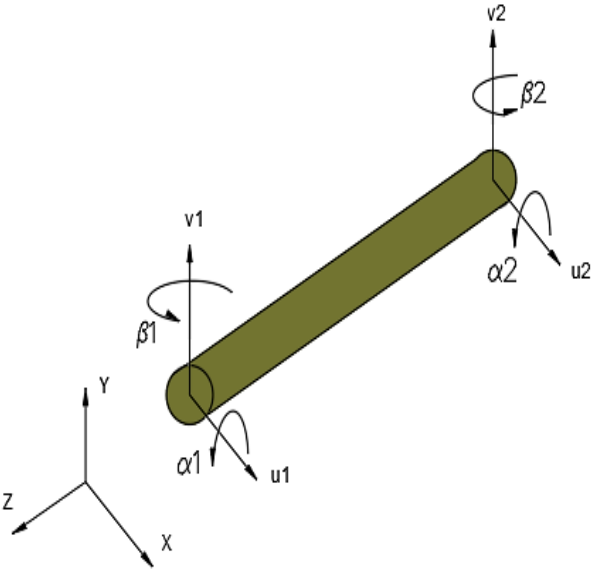

Fig. 2 Beam element representation.

where, u and v refer to translations in direction of x and y respectively while α and β refer to rotation about x and y axes respectively. The mass, stiffness, and gyroscopic matrices for the beam element are provided from [28].

The beam element stiffness matrix is identified by:[28]

$$\boldsymbol{K}_{ele} = \frac{EI}{(1+\varphi)l^3}\begin{bmatrix} 12 & 0 & 0 & 6l & -12 & 0 & 0 & 6l \\ 0 & 12 & -6l & 0 & 0 & -12 & -6l & 0 \\ 0 & -6l & (4+\varphi)l^2 & 0 & 0 & 6l & (2-\varphi)l^2 & 0 \\ 6l & 0 & 0 & (4+\varphi)l^2 & -6l & 0 & 0 & (2-\varphi)l^2 \\ -12 & 0 & 0 & -6l & 12 & 0 & 0 & -6l \\ 0 & -12 & 6L & 0 & 0 & 12 & 6l & 0 \\ 0 & -6l & (2-\varphi)l^2 & 0 & 0 & 6l & (4+\varphi)l^2 & 0 \\ 6l & 0 & 0 & (2-\varphi)l^2 & -6l & 0 & 0 & (4+\varphi)l^2 \end{bmatrix} \quad (6)$$

In the above matrix equation, ϕ refers to the shear constant, which reflects the shear flexibility of the beam, l is the length of the element of the beam, E expresses the modulus of elasticity, and I represents the second moment for the beam cross-section area. The generalized coordinate of each shaft element is expressed in the following sequence of the DoFs: $[\mu_1 v_1 \ \alpha_1\beta_1 \ \mu_2 v_2 \ \alpha_1\beta_2]$.

The mass matrix for the beam element is determined from [28].

$$\boldsymbol{M}_e = \frac{\rho Al}{840(1+\varphi)^2}\begin{bmatrix} M_{e1} & 0 & 0 & M_{e2} & M_{e3} & 0 & 0 & M_{e4} \\ 0 & M_{e1} & -M_{e2} & 0 & 0 & M_{e3} & -M_{e4} & 0 \\ 0 & -M_{e2} & M_{e5} & 0 & 0 & M_{e4} & M_{e6} & 0 \\ M_{e2} & 0 & 0 & M_{e5} & -M_{e4} & 0 & 0 & M_{e6} \\ M_{e3} & 0 & 0 & -M_{e4} & M_{e1} & 0 & 0 & -M_{e2} \\ 0 & M_{e3} & M_{e4} & 0 & 0 & M_{e1} & M_{e2} & 0 \\ 0 & -M_{e4} & M_{e6} & 0 & 0 & M_{e2} & M_{e5} & 0 \\ M_{e4} & 0 & 0 & M_{e6} & -M_{e2} & 0 & 0 & M_{e5} \end{bmatrix} \quad (7)$$

In the above matrix:

$$M_{e1} = 312 + 588\varphi + 280\varphi^2 \quad (8)$$

$$M_{e2} = (44 + 77\varphi + 35\varphi^2)l \quad (9)$$

$$M_{e3} = 108 + 252\varphi + 140\varphi^2 \quad (10)$$

$$M_{e4} = -(26 + 63\varphi + 35\varphi^2)l \quad (11)$$

$$M_{e5} = (8 + 14\varphi + 7\varphi^2)l^2 \quad (12)$$

$$M_{e6} = -(6 + 14\varphi + 7\varphi^2)l^2 \quad (13)$$

The matrix of the gyroscope for the beam element is calculated as:[28]

$$\boldsymbol{G}_e = \frac{\rho I}{15l(1+\phi)^2}\begin{bmatrix} 0 & -G_{e1} & G_{e2} & 0 & 0 & G_{e1} & G_{e2} & 0 \\ G_{e1} & 0 & 0 & G_{e2} & -G_{e1} & 0 & 0 & G_{e2} \\ -G_{e2} & 0 & 0 & -G_{e3} & G_{e2} & 0 & 0 & -G_{e4} \\ 0 & -G_{e2} & G_{e3} & 0 & 0 & G_{e2} & G_{e4} & 0 \\ 0 & G_{e1} & -G_{e2} & 0 & 0 & -G_{e1} & -G_{e2} & 0 \\ -G_{e1} & 0 & 0 & -G_{e2} & G_{e1} & 0 & 0 & -G_{e2} \\ -G_{e2} & 0 & 0 & -G_{e4} & G_{e2} & 0 & 0 & -G_{e3} \\ 0 & -G_{e2} & G_{e4} & 0 & 0 & G_{e2} & G_{e3} & 0 \end{bmatrix} \quad (14)$$

In the above matrix equation:

$$G_{e1} = 36 \quad (15)$$

$$G_{e2} = (3 - 15\varphi)l \quad (16)$$

$$G_{e3} = (4 + 5\varphi + 10\varphi^2)l^2 \quad (17)$$

$$G_{e4} = (-1 - 5\varphi + 5\varphi^2)l^2 \quad (18)$$

where ρ refers to the material density of the shaft, A is the cross-sectional area of the rotating shaft, and φ refers to the shear coefficient.

To model the bearings of the rotor system, the stiffness of the bearing is introduced as a spring-like element at a single node in the direction of bearing support. The outer damping is involved in the system using bearing support damping. Computing the matrices of mass, stiffness, and gyroscopic of the element will facilitate the assembling of the rotor system global matrices {M, D, K} mass, damping and stiffness matrices respectively. The contributions of the damping and stiffness from the bearings are then involved in the global matrices of the system.

The natural frequencies and mode shapes can then be determined using the assembled global {M, D, K} matrices. The matrix of state space companion of the system can be arranged as shown below:[28]

$$\boldsymbol{A} = \begin{bmatrix} 0 & \mathrm{I} \\ -\mathrm{M}^{-1}\mathrm{K} & -\mathrm{M}^{-1}\mathrm{D} \end{bmatrix} \quad (19)$$

The rotor system's natural frequencies and corresponding mode shapes are determined from the imaginary part of the eigenvalues and eigenvectors of the above matrix respectively. The rotor critical speeds were then determined.[27,28] It is well known that the critical rotational speed of a rotating shaft is the angular velocity that excites the natural frequency of the rotor. This critical speed (whirling) is relying on the shaft dimensions, material, and loads.

2.3 Numerical example

The computational model for the rotating machine developed in the current work is applied to a case study of a multi-disc rotor for the sake of verifying the reliability of the developed model. The FE model was implemented entirely using MATLAB. This rotating machinery comprises a horizontal flexible shaft fixed on two bearing supports with two rigid discs attached to the rotor, as shown in Fig. 3.

The rotor system FE model is demonstrated in Fig. 4. The length of the rotating shaft is 700 mm which was divided into 14 shaft elements. Consequently, 15 nodes with 4 DoFs at each node were generated. The details of the rotor model are defined in Tables 1 and 2.

In this study, three crack positions are considered. Position 1: The crack occurs close to the left bearing (50 mm distance from the left bearing support). Position 2: The crack appears away from the left bearing and before disc 1 (200 mm distance from the left bearing support). Position 3: A crack exists between the two discs (350 mm distance from the left bearing

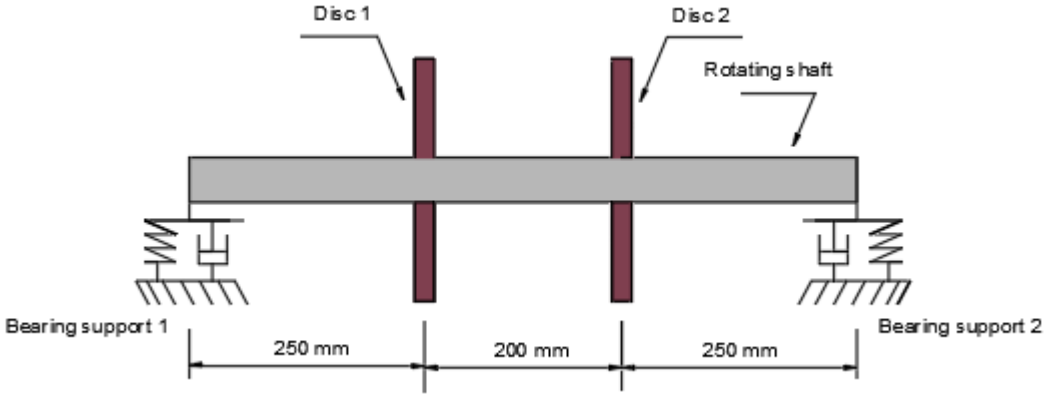

Fig. 3 Rotating machine model.

Table 1. Parameters of the rotor system model.

Elements number	14
Nodes number	15
DOFs	60
Bearings number	2 bearings located at nodes 1 and 15
Shaft diameter	20 mm
Stiffness of bearing	4 MN/m

Table 2. Material properties of the rotor shaft.

E : Young modulus	206 GPa
v : Poisson ratio	0.30
G : Shear modulus	$\frac{E}{2(1+v)}$
Density	7810 kg/m^3

support). In each position, various crack depths represented as a non-dimensional crack depth ratio are introduced. The crack depth ratio is defined as:

$$\delta = \frac{h}{D} \tag{20}$$

where δ is the crack depth ratio, h refers to the crack depth, and D denotes shaft diameter.

In this research, a wide range of crack depth ratios are dealt with for each crack position. The developed model has been used to identify the vibration responses, frequency response function (FRF), natural frequency and critical rotor speed. The results obtained for cracked and uncracked rotor shafts are compared to examine the influence of crack presence on the dynamic behavior.

3. Results and Discussion

The results obtained in this research are detailed in this section. Transient response, while the machine is running up to 5000 rpm, and steady-state vibration responses are analyzed for various sizes and locations of the cracks. The response measured is obtained in Y-direction (vertical) at disc 1. The results for maximum displacement responses over a wide range of crack depth ratios are presented in Fig. 5 for the three crack positions. It can be seen from this graph that crack position 1 has shown higher responses than the other two positions. Moreover, increasing the crack depth ratios resulted in decreasing the displacement response as the net cross-sectional area approached the critical size. However, the curve of the crack position 1 shows a slight increase before sharply

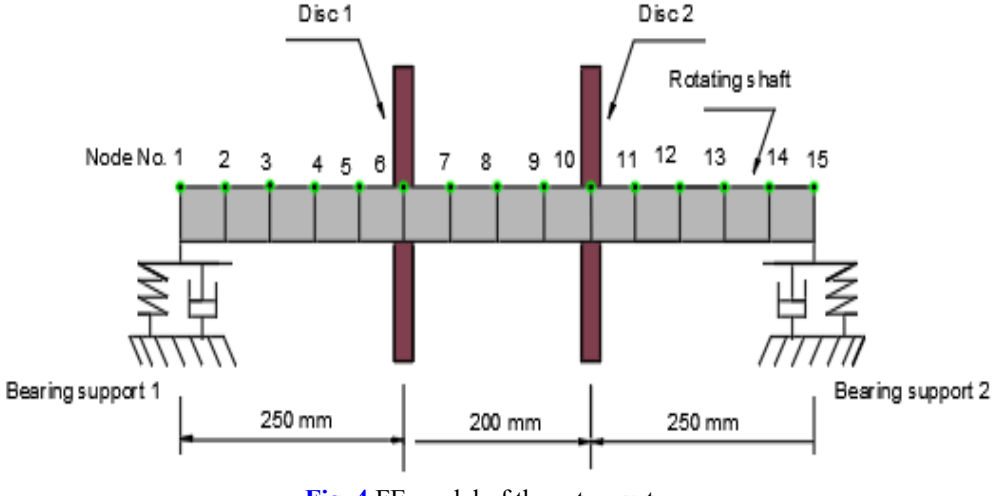

Fig. 4 FE model of the rotor system.

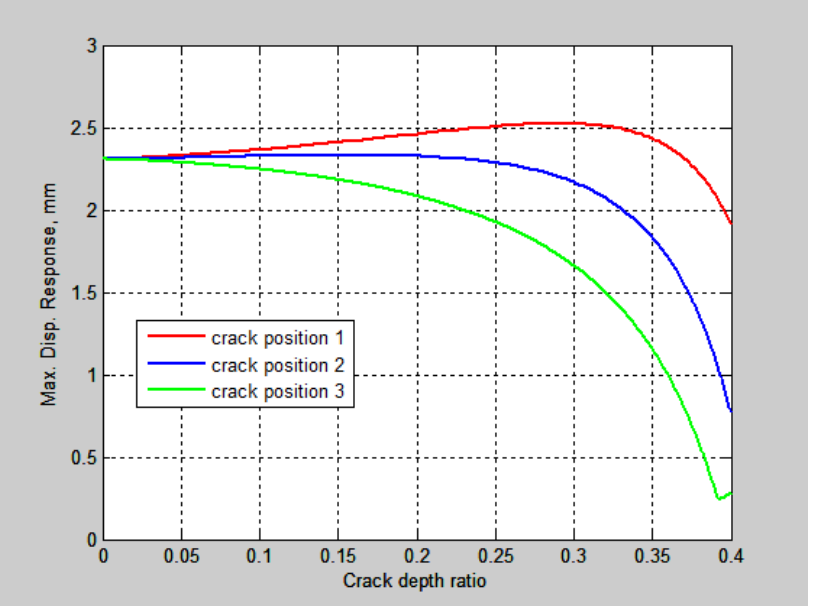

Fig. 5 Maximum transient displacement response for a wide range of crack depth ratios.

decreasing. On the other side, the decrease in maximum response at crack position 3 was more sensitive to crack depth than the other two positions.

The results obtained regarding the effect of crack depth and position on the rotor displacement response while machine run-up are presented in Fig. 6(a) to Fig. 8(a) for crack positions 1, 2, and 3 respectively. It can be seen from these graphs that as the crack depth increases the displacement response increases. However, as the crack depth approaches its critical size, the displacement response decreases in comparison with the uncracked shaft condition, as demonstrated more clearly in Figs. 6(b), 7(b), and 8(c). Regarding the effect of crack position, it is noticed that the displacement response for crack position 3 was higher than that for crack positions 2 and 1.

The results obtained for the influence of crack depth and position on the frequency response of the rotor during running up are shown in Fig. 9 to Fig. 11 for crack positions 1, 2, and 3 respectively. It is clear from these plots that the response amplitude increases as the crack depth increases compared with the case of uncracked rotor. Once again, it is found that as the crack depth approaches the critical size the response amplitude decreases in comparison with the uncracked case. In addition, this reduction in response amplitude for crack position 1 was higher than that for the other two positions, particularly at higher frequencies. Moreover, as the crack deepens, sub-resonances emerge in the transient responses, as shown in Fig. 8.

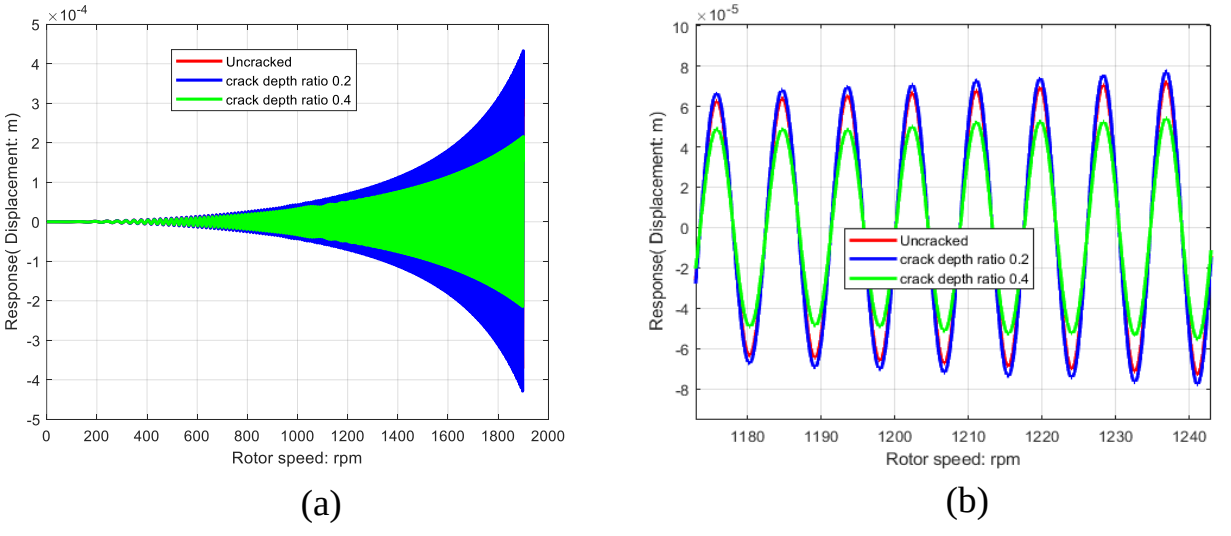

Fig. 6 (a) Transient displacement response during rotor running up for crack position 1, (b) Displacement response during rotor running up for crack position 1.

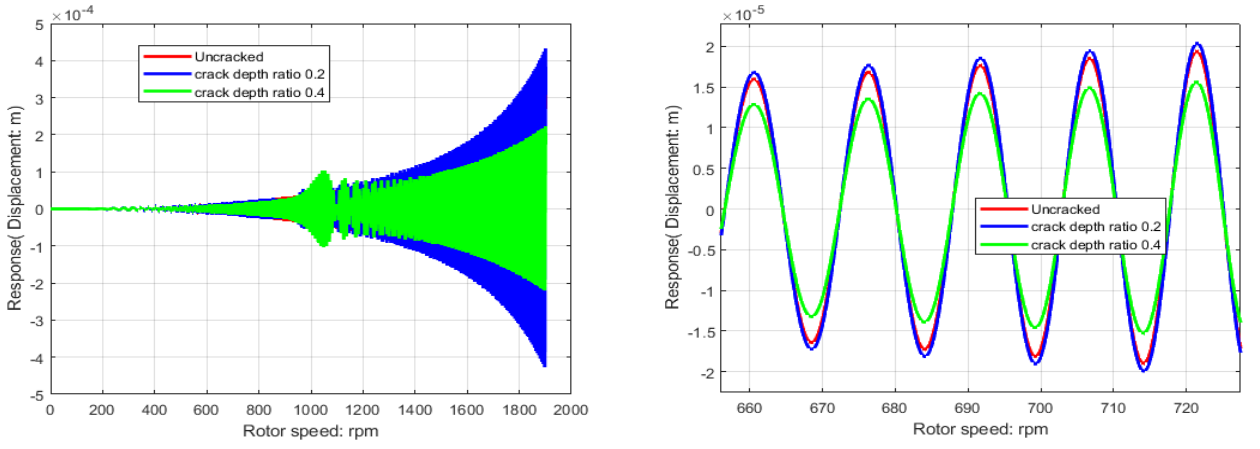

(a) (b)

Fig. 7 (a) Transient displacement response during rotor running up for crack position 2, (b) Magnified view for the response during rotor running up for crack position 2.

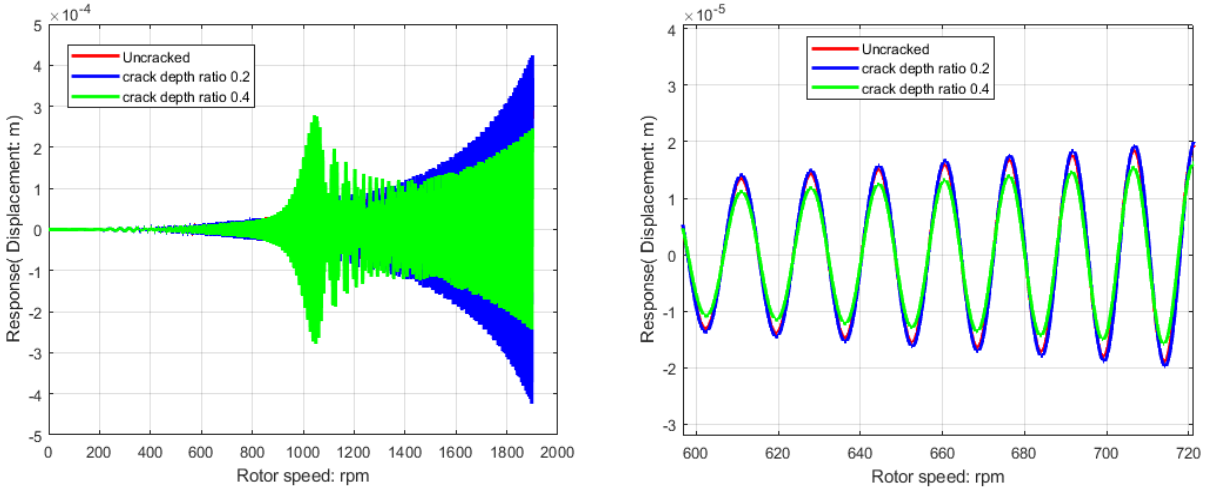

(a) (b)

Fig. 8 (a) Transient displacement response during rotor running up for crack position 3, (b) Magnified view for the response during rotor running up for crack position 3.

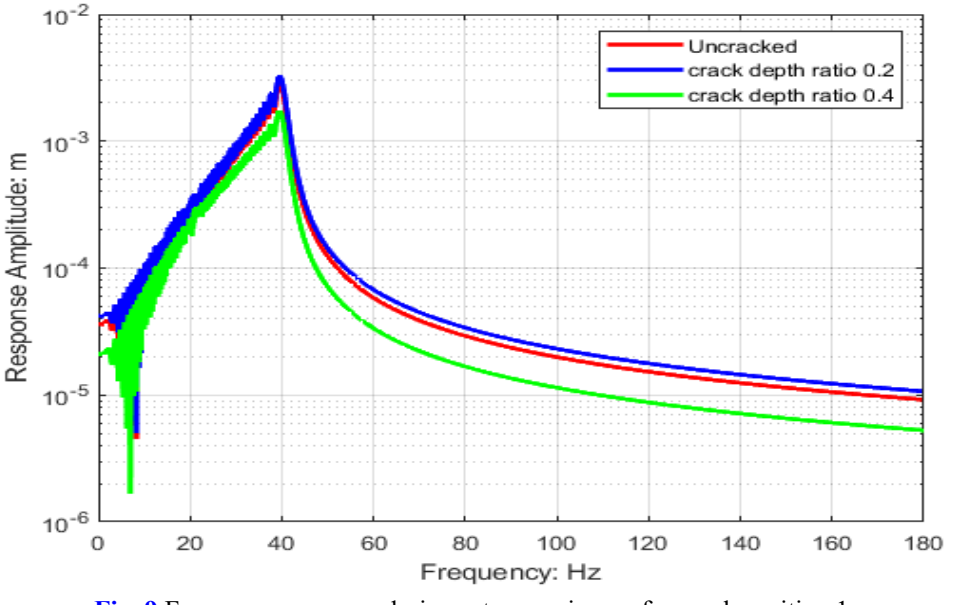

Fig. 9 Frequency response during rotor running up for crack position 1.

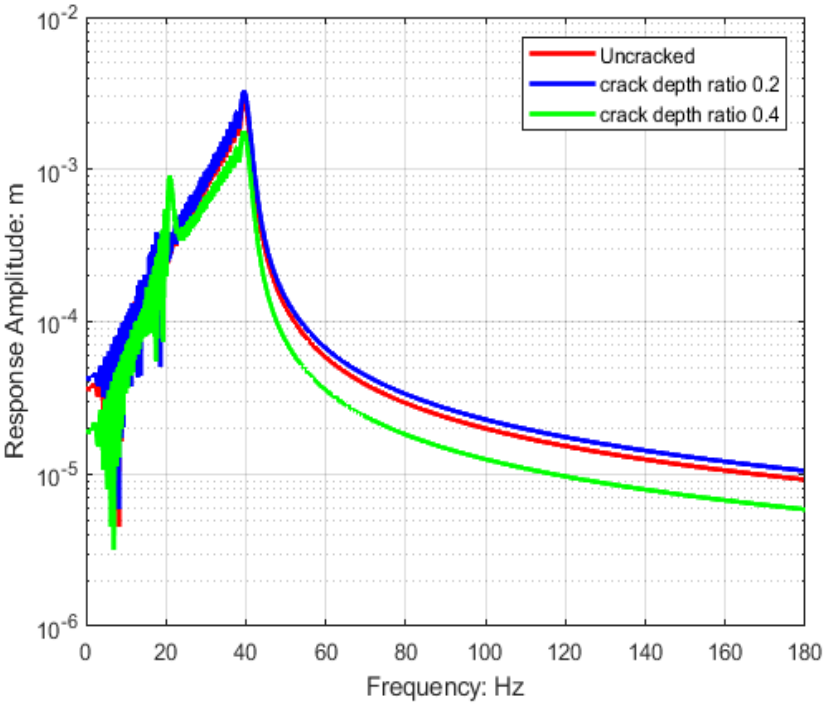

Fig. 10 Frequency response during rotor running up for crack position 2.

The influence of crack depth and position on the rotor critical speed for the three crack positions are presented in Fig. 12. It can be deduced from the plots shown in this graph that the critical speed of the rotor decreases as the crack deepens in comparison with the case of the rotor without crack. The decrease in critical speed of the rotor system is due to the reduction in the stiffness of the rotor, which results from the existence of the crack. However, the rate of this decrease is very low for low crack depth values, and then it increases for higher crack depths. Furthermore, the reduction in critical speed is related to the crack position, and the larger reduction was found in crack position 1. Therefore, one may conclude that the reduction in critical speed is higher as the crack location approaches the supporting bearing. The results obtained in the current study are compared with the available published results and findings in this respect, for example.[29-31] The comparison shows a good agreement, which verifies the approach developed in this study.

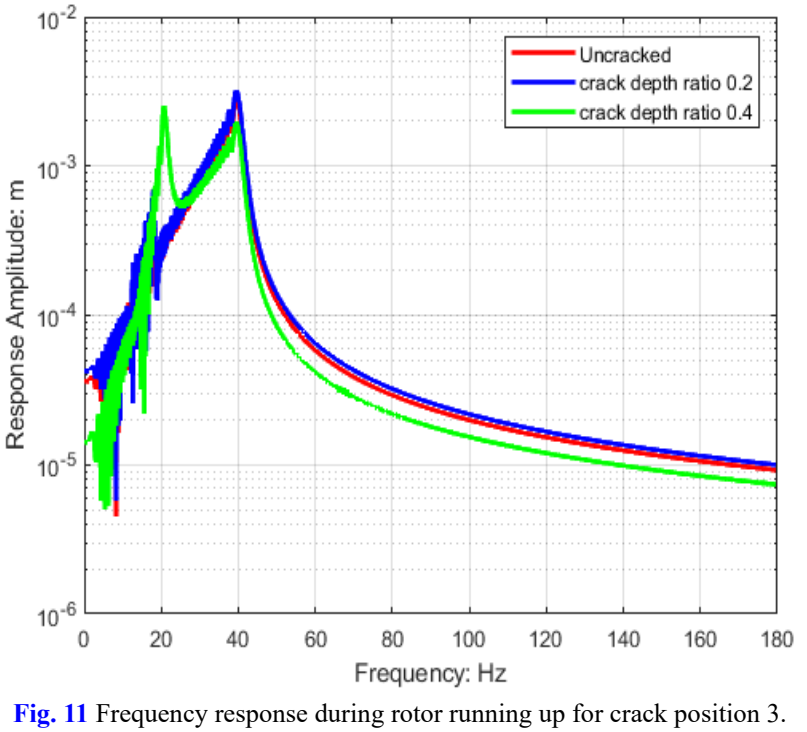

Fig. 11 Frequency response during rotor running up for crack position 3.

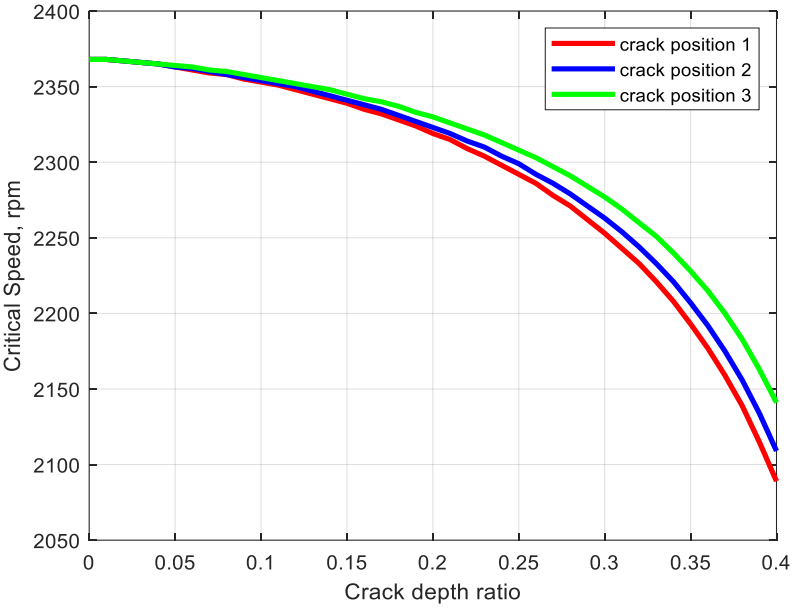

Fig. 12 Influence of crack depth and position on the rotor critical speed.

3.1 Experimental verification

This section presents the experimentation performed to validate the proposed approach developed in the current study. An actual rotor system was arranged according to the rotating machine model considered in this work. The experimental configuration setup is shown in Fig. 13. The test rig comprises a 20 mm diameter rotating shaft supported on two bearing supports with two attached discs having a diameter of 140 mm and thickness of 10 mm. The rotor system is driven using a motor, as shown in Fig. 13 below.

The impact hammer test procedure was conducted to extract the measured natural frequency of the rotating machine. This tap testing was implemented using an impact hammer as the excitation source and an accelerometer as the sensor, as well as using a suitable amplifier and oscilloscope. The accelerometer was installed at different locations on the test rig. The experiments were implemented to measure the natural frequency of the above machine. The corresponding critical speed was then found accordingly. As specified earlier, the experimental testing was conducted using cracked shafts with crack depth ratios for each crack position. Both first and second natural frequencies and critical speeds were measured for each case. Consequently, five shafts with the same diameter defined in the rotor model were tested. One uncracked shaft was tested to measure the original dynamic properties. The other four with a crack depth ratio of (0.1, 0.2, 0.3, and 0.4) were tested for crack positions 1, 2, and 3 to investigate the influence of crack existing on dynamic properties. The experimental results of the critical speed for the three crack positions are presented in Fig. 14. By comparing these results with those obtained numerically, shown in Fig. 7, a good agreement is obtained, which validates the developed model.

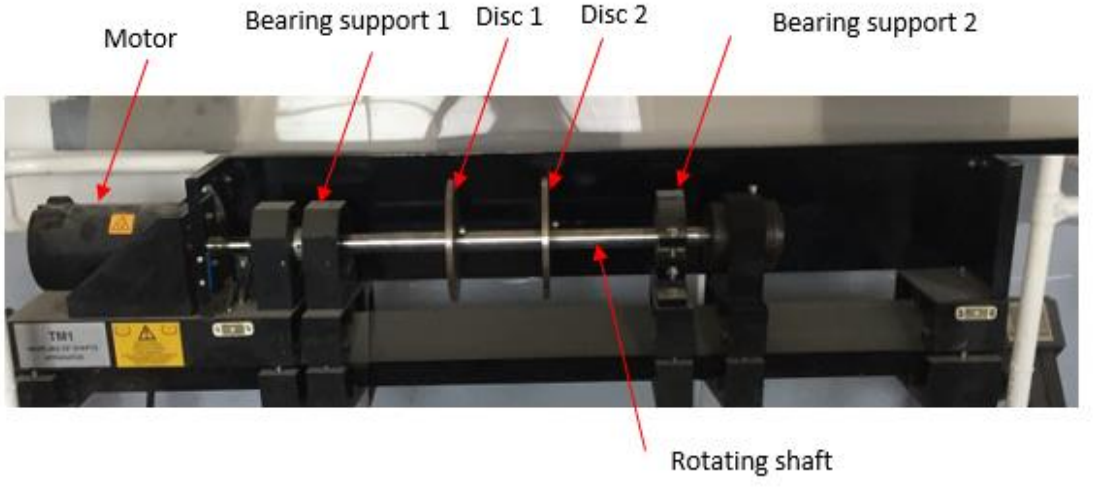

Fig. 13 Experimental setup of the rotating machine model.

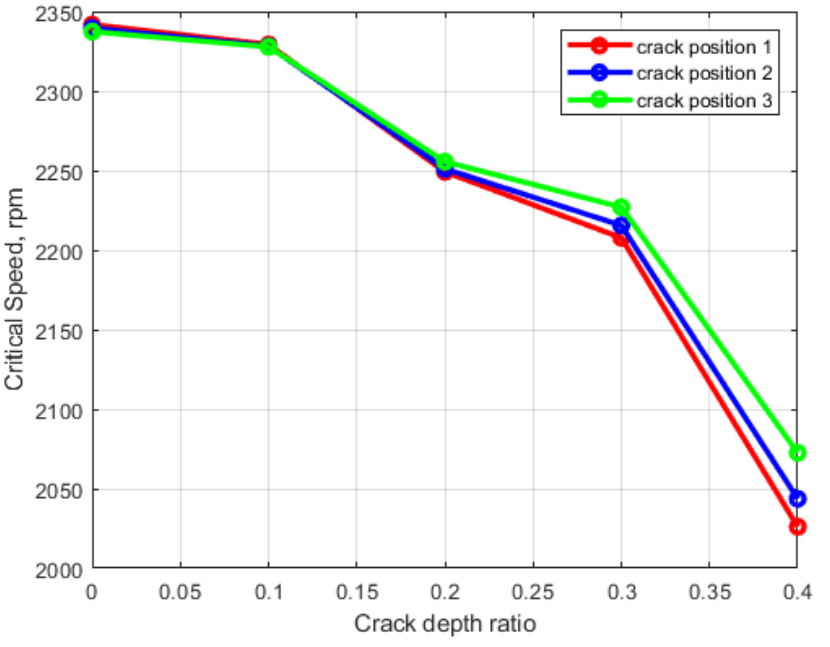

Fig. 14 Experimental results for the impact of crack depth and position on critical speed.

For the sake of comparison and to identify the maximum error between the results obtained from the numerical model and those obtained experimentally, the measured and numerical values of the rotor critical speed are plotted on same graph for crack positions 1, 2, and 3 as shown in Fig. 15 to Fig. 17 respectively. A good agreement has been obtained between the measured and experimental results with maximum error of a round 3%, 3.1%, and 3.2% at crack position 1, 2, and 3 respectively. This error is within a reasonable range, which verifies the numerical model developed in this study.

Finally, it is shown that the crack depth and position are important factors affecting the behavior of the rotating machine. In addition, the crack effect becomes more dangerous as its location is closer to bearing support due to the additional flexibility produced by the crack. Moreover, the crack reduces the critical speed of the rotor system and makes changes in the vibration responses, frequency and displacement responses as the crack presence weakens the rotor stiffness. Furthermore, it is evident that the sub-resonance level increases with the increase in the crack depth

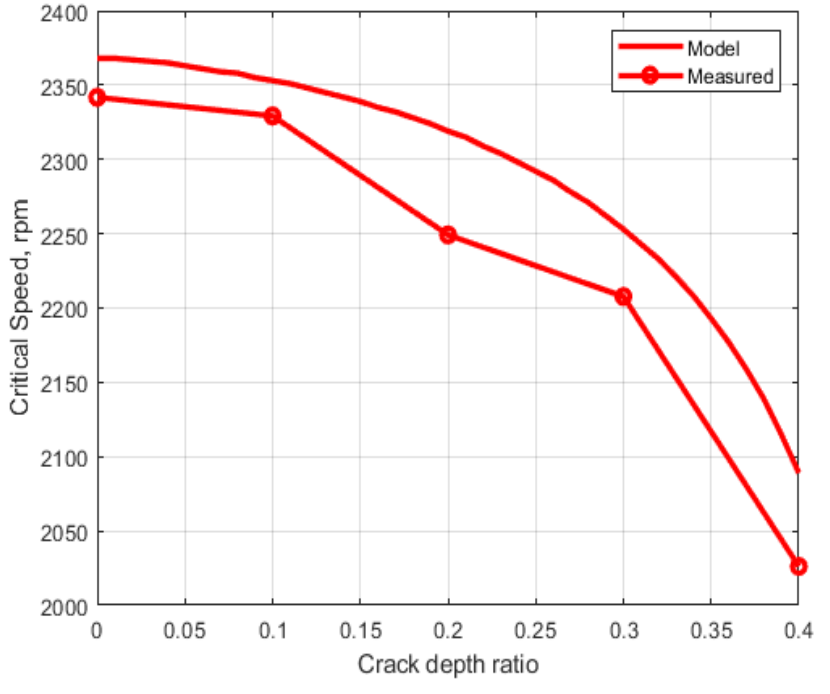

Fig. 15 Influence of crack depth on rotor critical speed at position 1.

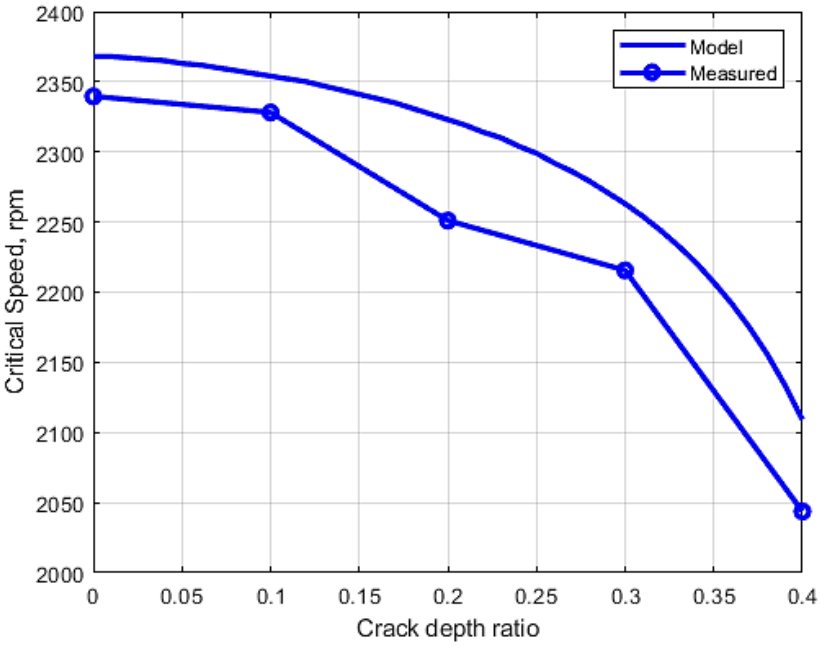

Fig. 16 Influence of crack depth on rotor critical speed at position 2.

for the running up responses. For the sake of validation, a comparison was also conducted with the results found from some of the available literature [23,26,31,32], and it is shown that the results obtained in this study agree well with those found in these papers.

4. Conclusions

In this paper, a muti-disc rotor system with a transverse crack was modeled through the FE displacement approach to investigate the dynamic behavior. The influence of crack position and depth on the dynamic characteristics involving critical speed, displacement and frequency responses as well as vibration responses were investigated under transient operation conditions. The following conclusions are derived from this study:

- A novel displacement–based FE model to investigate the dynamic behavior of multi-disc cracked rotating machines is proposed.
- The developed model was applied to a numerical case study example of a muti-disc rotor system with a transverse crack to demonstrate the performance of the proposed model.
- The influence of crack position and depth on the dynamic

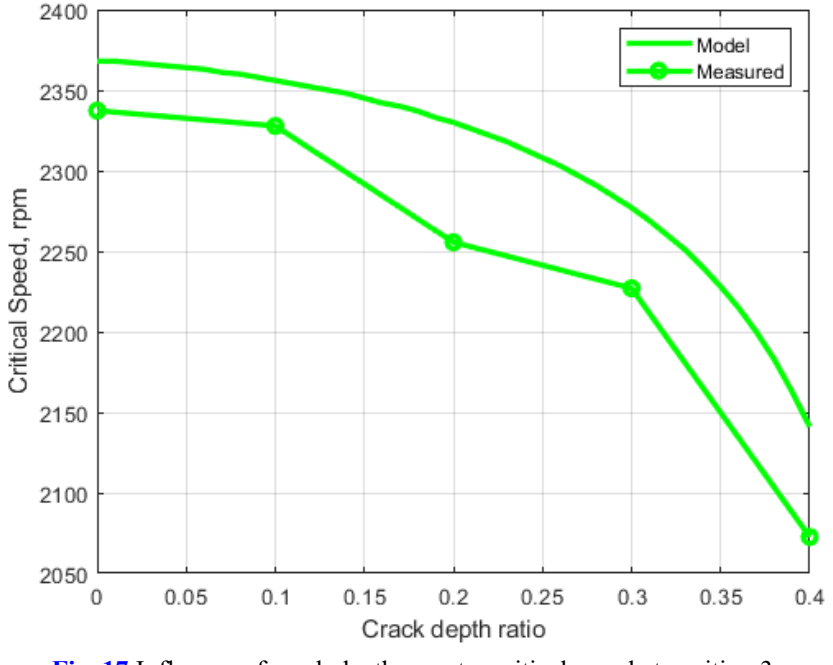

Fig. 17 Influence of crack depth on rotor critical speed at position 3.

characteristics involving critical speed, displacement and frequency responses as well as vibration responses were investigated under transient operation conditions.
- The developed model was validated experimentally through a test rig.
- Both numerical and experimental results demonstrate that the position and depth of the transverse crack reveal a noticeable impact on the dynamic behavior of the rotating machine.
- The results obtained indicate that the presence of crack leads to a remarkable change in vibration response, natural frequency, and critical speed. The amount and nature of this change were observed to be varying with crack depth and location.
- It was shown that the critical speed decreases as the crack deepens. Moreover, the crack effect on the dynamic of the rotor increases as the crack location is near the bearing support.
- Consequently, the suggested model introduces a possible approach for an online monitoring and diagnostic methods for rotating machines.

As future research, one may consider investigation of dynamic of FGM rotating shaft under such conditions dealt with in this paper.

Conflict of Interest

There is no conflict of interest.

Supporting Information

Not applicable.

References

[1] R. Tiwari, Rotor Systems: Analysis and Identification, CRC Press, 2017.
[2] G. Genta, Dynamics of rotating systems, 2007, doi: 10.1007/0-387-28687-X.
[3] Q. Xiong, H. Guan, H. Ma, Z. Wu, X. Guo, W. Wang, Dynamic characteristic analysis of rotating blade with breathing crack, *Mechanical Systems and Signal Processing*, 2023, **196**, 110325, doi: 10.1016/j.ymssp.2023.110325.
[4] Y. H. Park, H. B. Lee, G. W. Kim, Crack monitoring in rotating shaft using rotational speed sensor-based torsional stiffness estimation with adaptive extended Kalman filters, *Sensors*, 2023, **23**, 2437, doi: 10.3390/s23052437.
[5] Z. Li, Y. Li, D. Wang, Z. Peng, H. Wang, Dynamic characteristics of rotor system with a slant crack based on fractional damping, *Chinese Journal of Mechanical Engineering*, 2021, **34**, 1-18, doi: 10.1186/s10033-021-00543-w.
[6] Y. Yang, J. Wang, Y. Wang, C. Fu, Q. Zheng, K. Lu, Dynamical analysis of hollow-shaft dual-rotor system with circular cracks, *Journal of Low Frequency Noise, Vibration and Active Control*, 2021, **40**, 1227-1240, doi: 10.1177/1461348420948287.
[7] Z. Wan, Y. Wang, B. Chen, Y. Dou, X. Wei, The vibration of a transversely cracked rotor supported by anisotropic journal bearings with speed-dependent characteristic, *Applied Sciences*, 2020, **10**, 5617, doi: 10.3390/app10165617.
[8] D. Gayen, R. Tiwari, D. Chakraborty, Thermo-mechanical analysis of a rotor-bearing system having a functionally graded shaft with transverse breathing cracks. In Proceedings of the 6th National Symposium on Rotor Dynamics, Singapore: Springer, 2021.
[9] D. Gayen, D. Chakraborty, R. Tiwari, Stability behavior of two-crack functionally graded shaft in a rotor-disc system: finite element approach, *Materials Today: Proceedings*, 2020, **24**, 432-441, doi: 10.1016/j.matpr.2020.04.295.
[10] D. Gayen, D. C.hakraborty, R. Tiwari, Finite element analysis for dynamic response of rotor-bearing system with cracked functionally graded turbine shaft, *Gas Turbine India Conference*, 2017, **58516**, 7-8, doi: 10.1115/GTINDIA2017-4534.
[11] D. Gayen, D. Chakraborty, R. Tiwari, Whirl frequencies and critical speeds of a rotor-bearing system with a cracked functionally graded shaft–Finite element analysis, *European Journal of Mechanics - A*, 2017, **61**, 47-58, doi: 10.1016/j.euromechsol.2016.09.003.
[12] C. Z. Guo, J. H. Yan, L. A. Bergman, Experimental dynamic analysis of a breathing cracked rotor, *Chinese Journal of Mechanical Engineering*, 2017, **30**, 1177-1183, doi: 10.1007/s10033-017-0180-7.
[13] J. Penny, M. Friswell, The dynamics of cracked rotors. conference proceedings of the society for experimental mechanics series, 2007.
[14] J. J. Sinou, A. W. Lees, The influence of cracks in rotating shafts, *Journal of Sound and Vibration*, 2005, **285**, 1015-1037, doi: 10.1016/j.jsv.2004.09.008.
[15] C. Kumar, V. Rastogi, A brief review on dynamics of a cracked rotor, *International Journal of Rotating Machinery*, 2009, **2009**, 758168, doi: 10.1155/2009/758108.
[16] L. Hou, Y. Chen, Q. Cao, Z. Lu, Nonlinear vibration analysis of a cracked rotor-ball bearing system during flight maneuvers, *Mechanism and Machine Theory*, 2016, **105**, 515-528, doi: 10.1016/j.mechmachtheory.2016.07.024.
[17] Y. Ishida, Cracked rotors: industrial machine case histories and nonlinear effects shown by simple Jeffcott rotor, *Mechanical Systems and Signal Processing*, 2008, **22**, 805-817, doi: 10.1016/j.ymssp.2007.11.005.
[18] A. H. Kekan and B. R. Kumar, Critical speed and natural frequency analysis of cracked rotor shaft, *International Journal of Mechanical Engineering and Technology*, 2019, **10**, 232-240.
[19] J. M. Machorro-López, D. E. Adams, J. C. Gómez-Mancilla, K. A. Gul, Identification of damaged shafts using active sensing—simulation and experimentation, *Journal of Sound and Vibration*, 2009, **327**, 368-390, doi: 10.1016/j.jsv.2009.06.025.

[20] H. Peng, Q. He, The effects of the crack location on the whirl motion of a breathing cracked rotor with rotational damping, *Mechanical Systems and Signal Processing*, 2019, **123**, 626-647, doi: 10.1016/j.ymssp.2019.01.029.
[21] J. J. Sinou, A. W. Lees, The influence of cracks in rotating shafts, *Journal of Sound and Vibration*, 2005, **285**, 1015-1037, doi: 10.1016/j.jsv.2004.09.008.
[22] Y. Wei, S. Yang, W. Chen, J. Li, The influence of transverse cracks to propagation characteristics of elastic waves propagating in a non-uniform shaft, *Journal of Sound and Vibration*, 2019, **444**, 35-47, doi: 10.1016/j.jsv.2018.12.032.
[23] J. Zeng, K. Chen, H. Ma, T. Duan, B. Wen, Vibration response analysis of a cracked rotating compressor blade during Run-up process, *Mechanical Systems and Signal Processing*, 2019, **118**, 568-583, doi: 10.1016/j.ymssp.2018.09.008.
[24] C. Z. Guo, J. H. Yan, L. A. Bergman, Experimental dynamic analysis of a breathing cracked rotor, *Chinese Journal of Mechanical Engineering*, 2017, **30**, 1177-1183, doi: 10.1007/s10033-017-0180-7.
[25] L. Cheng, N. Li, X. F. Chen, Z. J. He, The influence of crack breathing and imbalance orientation angle on the characteristics of the critical speed of a cracked rotor, *Journal of Sound and Vibration*, 2011, **330**, 2031-2048, doi: 10.1016/j.jsv.2010.11.012.
[26] H. Khorrami, R. Sedaghati, S. Rakheja, Vertical transient response analysis of a cracked jeffcott rotor based on improved empirical mode decomposition, *Vibration*, 2022, **5**, 408-428, doi: 10.3390/vibration5030023.
[27] E. K. Armstrong, Rotordynamics prediction in engineering, *Proceedings of the Institution of Mechanical Engineers*, 1998, **212**, 299.
[28] Z. Shen, B. Chouvion, F. Thouverez, A. Beley, Enhanced 3D solid finite element formulation for rotor dynamics simulation, *Finite Elements in Analysis and Design*, 2021, **195**, 103584, doi: 10.1016/j.finel.2021.103584.
[29] B. Muñoz-Abella, L. Montero, P. Rubio, L. Rubio, Determination of the critical speed of a cracked shaft from experimental data, *Sensors*, 2022, **22**, 9777, doi: 10.3390/s22249777.
[30] Y. Jin, L. Hou, Y. Chen, Z. Lu, An effective crack position diagnosis method for the hollow shaft rotor system based on the convolutional neural network and deep metric learning, *Chinese Journal of Aeronautics*, 2022, **35**, 242-254, doi: 10.1016/j.cja.2021.09.010.
[31] L. S. Leão, A. A. Cavalini Jr, T. S. Morais, G. P. Melo, V. Steffen Jr, Fault detection in rotating machinery by using the modal state observer approach, *Journal of Sound and Vibration*, 2019, **458**, 123-142, doi: 10.1016/j.jsv.2019.06.022.
[32] Z. Yang, T. Hussain, A. A. Popov, S. McWilliam, Novel optimization technique for variation propagation control in an aero-engine assembly, *Proceedings of the Institution of Mechanical Engineers, Part B: Journal of Engineering Manufacture*, 2011, **225**, 100-111, doi: 10.1243/09544054jem2043.